Material Gain in Polar GaInN and AlGaN Quantum Wells: How to Overcome the 'Dead' Width for Light Emitters in These QW Systems?

Marta Gladysiewicz, Czesław Skierbiszewski, and Robert Kudrawiec

Abstract*—Polar GaInN and AlGaN quantum wells (QWs) are widely used in light emitting diodes and laser diodes (LDs). However, the widths of such QWs are usually limited to a few nanometers in order to ensure a sufficiently large overlap between the wave functions of the ground electron and the ground hole state. By increasing the QW width we enter the area of 'dead' width where, the overlap of the electron and hole wave functions decreases almost to zero and the luminescence efficiency drastically deteriorates. Therefore, it is assumed that wide QWs are not suitable for light emitters and very wide (8-15 nm) QWs are not considered as a promising gain medium for LDs. Hence such QWs are very rarely studied both experimentally and theoretically. In this work the material gain is calculated for $Ga_{0.8}In_{0.2}N$/GaN and $Al_{0.8}Ga_{0.2}N$/AlN QWs with a width varying in the range of 2-15 nm. We observed that the material gain at fixed carrier concentration for these QWs drops to zero with the increase in the QW width and reaches negative values in the width range of ∼4-8 nm even for high carrier concentrations, but after exceeding a certain width to ∼8-12 nm it begins to increase rapidly and reaches the values greater than those observed for narrow QWs. This phenomenon is related to the screening of the built-in electric field by carriers, which is easier for wide QWs, and the reduction of the distance between the energy levels for electrons and holes. For the latter reason, optical transitions between higher energy states make a very significant contribution to the positive material gain.

***Index Terms*—Material gain, modeling, quantum wells, III-N.**

I. Introduction

THE SPONTANEOUS and piezoelectric polarization in wurtzite III-nitrides is extremely large [1], [2] and therefore this material aspect is very important in the design of optoelectronic devices. In general, the polarization phenomena can be beneficial in many semiconductor devices because they enabled interesting physical effects, such as doping-free high electron mobility transistors [3]–[6], polarization-induced doping [7], or enhancement in the tunneling current in devices with tunnel junctions [8]–[10]. However, they are rather not considered favorable in the GaInN and AlGaN quantum wells (QWs) used in light emitting diodes (LEDs) and laser diodes (LDs).

III-Nitride LEDs and LDs had found many applications including general lighting and displays [11]–[14], and more recently UV emitters [15]–[20], for which quantum efficiency is still low [18], [20]. Due to the possibility of inactivation of the coronavirus with UV-C light, this spectral range is becoming more and more interesting for both LEDs and LDs [21]. A successful realization of electrically pumped UV LDs has been reported by a several groups [20], [22]–[27], but performances of these devices are still unsatisfactory. Important challenges for the successful realization of UV-C LDs include several aspects [20] related to *i)* the presence of high dislocation densities, *ii)* very ineffective *p*- and *n*-type conduction in Al-rich AlGaN claddings, *iii)* inefficient light extraction from the active region, and *iv)* the non-optimized active region in terms of the material gain. The last challenge relates to polarization effects. These effects are also very important for GaInN QWs, which are used in the blue-green spectral region where efficient LDs exist but there is still room to improve the performance of these LDs.

The common challenge for GaInN and AlGaN QWs is the electric field engineering. Due to the spontaneous and piezoelectric polarization in III-Nitrides and the lattice mismatch between alloys forming the QW, a strong built-in electric field is present in GaInN and AlGaN QWs. Because of this a pronounced quantum confined Stark effect is present, leading to a red-shift of the emission spectra and spatial separation of electron and hole wave functions [28]–[34]. The latter is very unwanted phenomenon in both LEDs and LDs since it causes a significant reduction of the wave function overlap. For LEDs it leads to an increase in the carrier density at a given current flow through LED because of a lower probability of carrier recombination. It causes the reduction of quantum efficiency as a growing part of the carriers recombine through the nonradiative Auger process when the carrier density increases [35]–[39]. For LDs the material gain decreases with the increase in QW width because of the

Manuscript received April 7, 2021; revised June 17, 2021, July 29, 2021, and September 8, 2021; accepted September 19, 2021. Date of publication September 22, 2021; date of current version October 8, 2021. This work was supported by the National Science Centre, Poland, under Grant 2016/21/B/ST7/01274. (*Corresponding author: Marta Gladysiewicz.*)

Marta Gladysiewicz is with the Department of Experimental Physics, Faculty of Fundamental Problems of Technology, Wroclaw University of Science and Technology, 50-370 Wrocław, Poland (e-mail: marta.gladysiewicz@pwr.edu.pl).

Czesław Skierbiszewski is with the Institute of High Pressure Physics, Polish Academy of Sciences, 01-142 Warsaw, Poland (e-mail: czeslaw@unipress.waw.pl).

Robert Kudrawiec is with the Department of Semiconductor Materials Engineering, Faculty of Fundamental Problems of Technology,Wroclaw University of Science and Technology, 50-370 Wrocław, Poland, and also with the LUKASIEWICZ Research Network, PORT Polish Center for Technology Development, 54-066 Wroclaw, Poland (e-mail: robert.kudrawiec@port.lukasiewicz.gov.pl).

Color versions of one or more figures in this article are available at https://doi.org/10.1109/JSTQE.2021.3114316.

Digital Object Identifier 10.1109/JSTQE.2021.3114316

decrease of electron-hole overlap and therefore wide QW are not considered as a promising gain medium for LDs. In the case of GaInN/GaN QWs, the higher the indium content, the larger the built-in electric field related to piezoelectric polarization, and thus the larger the separation of carrier wave functions. This is the main cause of the loss of performance of GaInN QW devices in the green spectral range [12], [40]. In general, the same trend is expected for AlGaN/AlN QWs but this QW system is less explored.

Summarizing, very thin GaInN [11] and AlGaN [22]–[26], [41]–[44] QWs are utilized in LDs since a compromise between good quantum confinement and the large electron-hole overlap is present for 1.5-2.5 nm wide QWs [45]. For wider QWs (3-6 nm) low efficiency of emission is observed and therefore they are rarely used in LDs. 8-12 nm wide QWs (i.e., QW widths typical for LDs with non-polar QWs, i.e., GaAs-, InP-, and GaSb-based LDs [46]–[49]) are almost unexplored since it is usually assumed that such QWs will be worse for LDs applications that 3-6 nm wide QWs. However, it has recently been shown that wide GaInN QWs show unexpectedly strong photoluminescence under high excitation conditions [50] and LDs with such QWs work very well [51]. Therefore, it is a very interesting issue to carefully study material gain for GaInN and AlGaN over a wide range of widths. So far, gain calculations have been reported for GaInN and AlGaN QWs in several articles [45], [52]–[59], but for wide QWs such calculations have not been reported in these articles. The widest QWs, for which optical gain calculations have been reported so far, are the 9 nm AlGaN wells [60]. Therefore this is still unexplored area for polar QWs and this area is the subject of this article. We show that the material gain for polar GaInN/GaN and AlGaN/AlN QWs changes very unusually with the increase in QW width. A positive material gain disappears with the increase in QW width and appears again for 8-12 nm wide QWs due to the screening of the built-in electric field by carriers and the reduction of the distance between electron (hole) levels. It shows that due to the spontaneous and piezoelectric polarization in III-nitrides, the optimal QW width for applications in LDs is very unintuitive and very different from what is assumed to be optimal for non-polar QWs.

II. Theoretical Approach

The electronic band structure of GaInN/GaN and AlGaN/AlN QWs is calculated using ***kp*** Hamiltonian, which is given in details in Ref. [45]. The interaction between the CB and the VB is neglected because of the large band gap of GaInN and AlGaN, i.e., the calculation problem is reduced to the effective-mass Hamiltonian for the CB and the 6-band ***kp*** Hamiltonian for the VB. The Hamiltonian for VB is consistent with that used by other authors [52]–[54], [56], [61]–[63].

The band gap of GaInN and AlGaN is calculated using the parabolic formula with the bowing parameter of 1.7 and 0.7 eV, respectively [64]. The valence band offset (VBO) between GaInN (AlGaN) and GaN (AlN) is defined for unstrained materials, see Ref. [45]. A linear interpolation is used to obtain the valence band position in ternary alloys (GaInN and AlGaN) with the VBO for binary compounds (InN, GaN and AlN) taken from Ref. [64].

The influence of the compressive strain in GaInN and AlGaN layer on the electronic band structure in these alloys is calculated according to the Bir-Pikus model [65], details can be found in Ref. [45].

The electric field in the GaInN (AlGaN) QW and GaN (AlN) barriers is calculated according to periodic boundary conditions [30] (1)

$$F_n = \frac{\sum_q \frac{l_q P_q}{\varepsilon_q} - P_n \sum_q \frac{l_q}{\varepsilon_q}}{\varepsilon_n \sum_q \frac{l_q}{\varepsilon_q}} \tag{1}$$

where the sum runs over all the layers. ε_q, P_q, and l_q are the dielectric permittivity, total polarization, and width of the q-th layer, respectively. A QW with this electric field is the starting point in the self-consistent solution of the Schrödinger and Poisson equations [45]. The well-known Newton-Rhapson method was used to solve the Poisson equation and plane wave expansion methods were used to diagonalize the ***kp*** Hamiltonian. The total polarization is given by (2)

$$P_n = P_n^S + P_n^P, \tag{2}$$

where ${P_n}^S$ and ${P_n}^P$ mean the spontaneous and piezoelectric polarization in n-th layer, respectively. The piezoelectric polarization was calculated using (3).

$$P^p = \left(e_{31} - e_{33}\frac{c_{13}}{c_{33}}\right)\ (\in_{xx} + \in_{yy}) \tag{3}$$

c_{13} and c_{33} are the elastic constants, ϵ_{xx} and ϵ_{yy} are strains defined as: $\epsilon_{xx} = \epsilon_{yy} = (a_0\text{-}a)/a$, where a_0 and a are the lattice constants of the GaN (AlN) substrate and the GaInN (AlGaN) layer, respectively.

The piezoelectric tensor components (e_{31} and e_{33}), elastic constants (c_{13} and c_{33}), and other material parameters in GaInN and AlGaN alloys are determined using the linear interpolation of the binary parameters. Parameters of binary semiconductors used in our calculations are taken from the review paper on material parameters in III-N [64]. In recent years, some parameters have been updated [66] but they do not change much, so we decided to take the material parameters from one source for this study, with the exception of the parameters needed for the calculation of the polarization effects, which were carefully analyzed in Refs. [66], [67] and are taken into our calculations from [67].

The material gain for GaInN and AlGaN QWs is calculated for a given carrier density in QW region. This density in the CB and VB is calculated by the integration of product of the occupation probability of carriers (i.e., the Fermi-Dirac distribution) and the density of states, $\rho(k)$, over the entire band. The Fermi-Dirac distribution for electrons (f_{CB}) and holes (f_{VB}) in the QW is given by (4) and (5)

$$f_{CB}\ \left(E_{CB}\left(k\right), E_{CB}^F\right) = \left(1 + \exp\left(\frac{E_{CB}\left(k\right) - E_{CB}^F}{k_B T}\right)\right)^{-1}, \tag{4}$$

$$f_{VB}\left(E_{CB}(k), E_{CB}^F\right) = \left(1 + \exp\left(\frac{E_{VB}(k) - E_{VB}^F}{k_B T}\right)\right)^{-1}, \tag{5}$$

where k_B is the Boltzmann's constant and T is the temperature. Note that the carrier density determines the quasi-Fermi levels E_{CB}^F and E_{VB}^F for the CB and VB, respectively, and vice versa. The carrier density in conduction (*N*) and valence (*P*) band is calculated according to (6) and (7)

$$N = \sum_{n_{CB}} \int_0^{k_{max}} \rho(k)\, f_{CB}\left(E_{n_{CB}}(k), E_{CB}^F\right)\, dk \tag{6}$$

$$P = \sum_{n_{VB}} \int_0^{k_{max}} \rho(k)\left[1 - f_{VB}\left(E_{n_{VB}}(k), E_{VB}^F\right)\right]\, dk \tag{7}$$

The integration is carried out in *k* space with the density of states taken from ***kp*** calculations. k_{max} is the integration limit determined by convergence of integrals given by (6) and (7). The average carrier density is the input parameter that determines the position of the quasi-Fermi levels. Calculations are performed with a set number of levels in the conduction and valence band, i.e., 10 levels in CB and 20 levels in VB. The level that is considered bound in the QW is counted differently from the level that came out of it. In fact, the number of carriers in QW corresponding to the two-dimensional sheet density and three-dimensional conditions is calculated to correspond to the nominal value of average carrier density.

In this approximation the TE and TM mode of the material gain is given by (9):

$$g_{\beta_{\mathrm{TE(TM)}}}(\hbar\omega) = C_0\,\beta^{-1} \sum_{n_{CB},\, n_{VB}} \int dk\,(f_{n_{CB}}(k) - f_{n_{VB}}(k)) \sum_{i,j} |M|^2_{iCB-jHH_{\mathrm{TE(TM)}}}\, L(n_{CB}, n_{VB}, k) \tag{8}$$

where $C_0 = q^2/(\omega {m_0}^2 \tau_b c \varepsilon_0)$ (*q*–elementary charge; ω – angular frequency, m_o – electron mass; τ_b – broadening time; *c* – speed of light; ε_0 – dielectric constant), *i* and *j* represents, respectively, the electron and hole subbands, β in this case is the propagation constant of the TE (TM) mode, $|M|^2_{iCB-jVB_{\mathrm{TE(TM)}}}$ is the matrix element of TE (TM) mode, see details in Ref. [45]. This is a method based on the relaxation time approximation convoluted with a Lorentzian function given by (8)

$$L(n_{CB}, n_{VB}, k) = \frac{\hbar/\tau_b}{\Delta(n_{CB}, n_{VB}, k)^2 + (\hbar/\tau_b)^2}, \tag{9}$$

where Δ is the proper energy difference and $\hbar$ is the Planck constant divided by 2π. The broadening time $\tau_b = 0.1$ ps [45] is applied in our calculations to obtain the material gain spectra.

Our calculations do not take into account the inhomogeneous broadening and the excitonic effects. Typically, the excitonic effects are ignored in the gain calculations, but inhomogeneous broadening can be taken into account [60]. In this case, it is worth noting that this broadening can vary significantly with QW width due to the different sensitivity to interface roughness. Therefore, for this study, the choice of the same Lorentzian broadening is a compromise solution that does not affect the final conclusions.

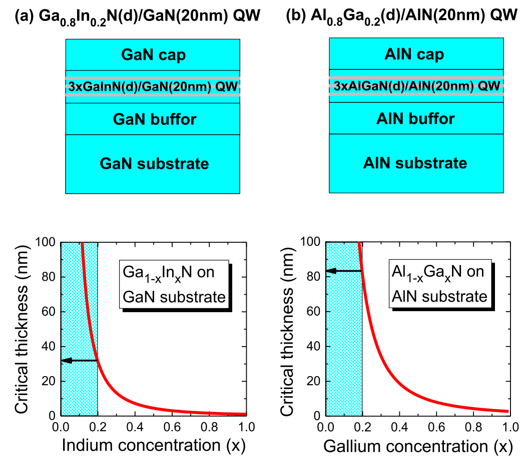

Fig. 1. Layer sequences in (a) $Ga_{0.8}In_{0.2}N(d)/GaN$ and (b) $Al_{0.8}Ga_{0.2}N(d)/AlN$ QWs together with the critical thickness for $Ga_{1-x}In_xN$ strained on GaN and $Al_{1-x}Ga_xN$ strained on AlN.

Fig. 1 shows the sketch of $Ga_{0.8}In_{0.2}N/GaN$ and $Al_{0.8}Ga_{0.2}N/AlN$ QWs of different width *d*, which are considered in this work. In addition, the critical thickness for $Ga_{1-x}In_xN$ ($Al_{1-x}Ga_xN$) layer grown on GaN (AlN) substrate is calculated according to Fisher's formula [68] and plotted in this figure.

In our calculations the QW width was varied from 2 to 15 nm, which is well below the critical thickness in the case of a single QW and also below the critical thickness in the case of multiple QWs if their number is properly low.

III. Results and Discussion

Fig. 2 shows spectra of the TE mode of material gain calculated for $Ga_{0.8}In_{0.2}N/GaN$ QWs of different widths at two carrier concentrations, i.e., 1.5 and 2.0×10^{19} cm^{-3}. The same three-dimensional carrier concentrations were chosen for this comparison, this concentration can be compared with the current that flows through the QW located in the *p-n* junction, since the laser output power is usually measured as a function of current [16], [17], [24], [26]. In general, the selected carrier concentrations in QW region are quite high and a positive material gain appears at much lower carrier concentrations for thin and wide QWs, but higher carrier concentrations are better to study changes in spectral position of the material gain and its intensity. It is clearly visible that as the width of QW increases, the gain peak shifts towards longer wavelengths and its intensity decreases, reaching negative values for the width of ~6-7 nm. A further increase in the QW width causes the appearance of a positive gain peak, its shift towards shorter waves and an increase in its intensity. The blue shift of gain peak is observed up to a width of ~10 nm, and a further increase in QW width does not significantly affect the peak position. The changes observed in the material gain spectra can be explained by the screening of the electric field in the analyzed QWs.

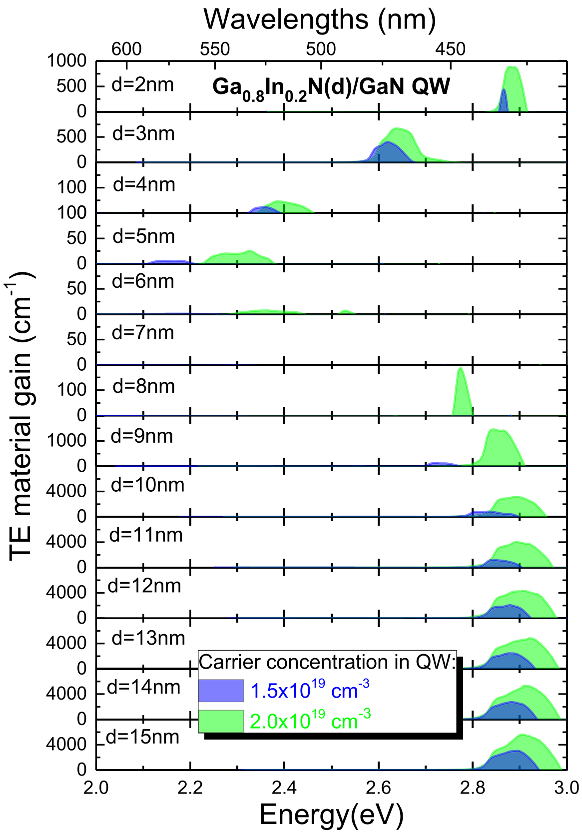

Fig. 2. TE mode of material gain for $Ga_{0.8}In_{0.2}N(d)/GaN$ QWs of different width at carrier concentration of 1.5 and 2.0 $\times$ 10^{19} cm^{-3}. The QW width is changing from 2 to 15 nm. The two-dimensional concentration of carriers in QW going from top to bottom is as follows: 3.0, 4.5, 6.0, 7.5, 9.0, 10.5, 12.0, 13.5, 15.0, 16.5, 18.0, 19.5, 21.0, 22.5 $\times 10^{12}$ cm^{-2} for the three-dimensional carrier concentration of 1.5×10^{19} cm^{-3} and 4.0, 6.0, 8.0, 10.0, 12.0, 14.0, 16.0, 18.0, 20.0, 22.0, 24.0, 26.0, 28.0, 30.0 $\times 10^{12}$ cm^{-2} for the three-dimensional carrier concentration of 2.0×10^{19} cm^{-3}.

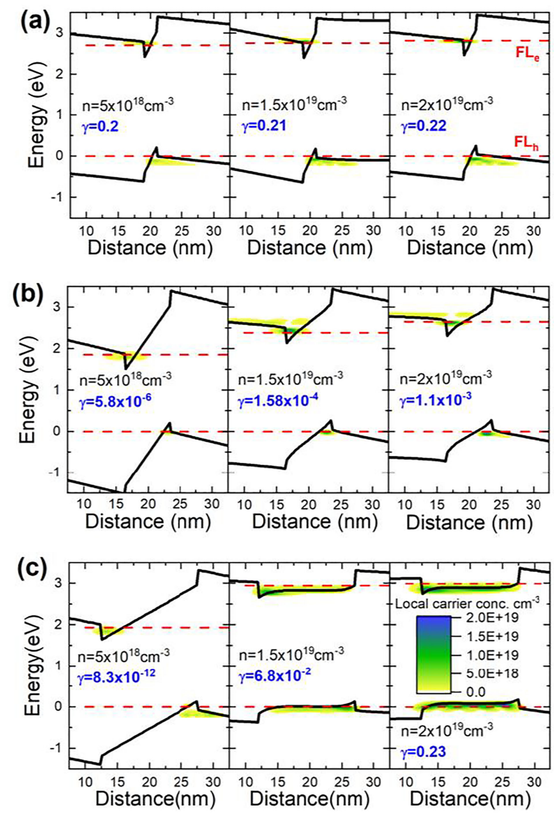

Fig. 3. The quantum confinement potential for (a) 2 nm, (b) 7 nm, and (c) 15 nm wide $Ga_{0.8}In_{0.2}N/GaN$ QWs obtained for different carrier concentrations in QW region. γ is the electron-hole overlap for the fundamental transition. FL_e and FL_h corresponds to the quasi Fermi level for electrons and holes, respectively. The color map shows the local carrier concentration at the appropriate energy levels. The total polarization discontinuity at the $Ga_{0.8}In_{0.2}N/GaN$ interface is 0.036 C/m^2 (it corresponds to the sheet concentration of 2.3×10^{13} cm^{-2}) and do not change with the QW width, while the redistribution of carriers within QWs of different width varies very significantly. The two-dimensional concentration of carriers in QW is as follows: (a) 1.0, 3.0, 4.0 $\times 10^{12}$ cm^{-2}; (b) 3.5, 10.5, 14.0 $\times 10^{12}$ cm^{-2}; (c) 7.5, 22.5, 30.0 $\times 10^{12}$ cm^{-2}.

Fig. 3 shows the confinement potential for $Ga_{0.8}In_{0.2}N/GaN$ QWs of different widths (2, 7, and 15 nm) under different carrier concentrations. The quasi Fermi-levels for electrons and holes are plotted in Fig. 3 as horizontal dashed lines and the energy scale is set to zero in this figure at the hole quasi Fermi-level. The color map corresponds to the carrier distribution depending on the location and energy. The appropriate colors correspond to different values of carrier concentration. When the local concentration is summed after energy and integrated at a distance and finally divided by the QW width, the nominal value of average carrier concentration is obtained. The distribution of concentration shows how the levels are occupied and how they are responsible for screening the electric field.

The total polarization discontinuity at interfaces in these QWs is 0.036 C/m^2, which corresponds to the sheet concentration of 2.3×10^{13} cm^{-2}. Comparing this concentration with the concentration of the two-dimensional carriers in QW, see the values given in the figure caption in Fig. 3, it is clear that the screening of the built-in electric field occurs when the concentration of the 2D carriers begins to be comparable to the sheet concentration. For narrow QWs the electron-hole overlap (γ) for the fundamental transition is significant even for low carrier concentration and does not change significantly with the increase in carrier concentration, see Fig. 3(a) for 2 nm wide $Ga_{0.8}In_{0.2}N/GaN$ QW. In this case electrons and holes are not able to separate in the growth direction and screen the built-in electric field. However such conditions are favorable for light emission since the electron-hole overlap is large in broad range of carrier concentrations. Therefore, the material gain is positive even for low carrier concentration in the QW region as will be shown in the next part of this paper.

For 7 nm wide QW the carrier separation in the growth direction is very large and the electron-hole overlap for the ground state transition is close to zero. With the increase in carrier concentration the electron-hole overlap does not increase significantly, see the γ parameter in Fig. 3(b). It explain why a positive material gain is not observed for this QW even if the quasi Fermi-level for electrons and holes is above the ground level. It is worth commenting here that in the case of electrons this level is much above the ground state than in the case of holes due to the lower effective mass for electrons.

The results for the 7 nm wide QW may not be promising in studies of wider QW, but as already shown in Fig. 2, a positive material gain is unexpectedly observed for wider QWs. This phenomenon can be easily understood by analyzing the confinement potential profile for a 15 nm wide $Ga_{0.8}In_{0.2}N/GaN$ QW presented in Fig. 3(c). At low carrier concentration the electron-hole overlap is very small because of very strong carrier separation along the growth direction. However with the increase in carrier concentration in QW region the built-in electric field is screened and the electron-hole overlap for the ground state transition increases rapidly and may be greater than that observed for narrow QWs. Therefore, a broad positive gain peak is observed for wide QWs. The large broadening of the material gain peak results from the contribution of optical transitions between the excited states, which are separated by low energy due to the large width of this QW.

An important effect observed in Fig. 2 that is worth discussing again is the shift of the gain peak with the change of QW width. The redshift of this peak with an increase in QW width from 2 to 5 nm is a well-known quantum confinement Stark effect, while the blueshift observed with a further increase in QW width from 8 to 10 nm is due to the screening of built-in electric field. The wider QWs are already screened and therefore no shift in the gain peak is observed for these QW. The red and blue shift of the gain peak depend on the average carrier density in QW region (compare green and blue peaks in Fig. 2) and this phenomenon is related to both the screening of built-in electric field and the contribution of optical transitions between excited states to the gain peak.

The positive material gain observed for wide QW makes them very interesting for LD applications. Therefore, it is interesting to compare the material gain at different carrier concentrations for QWs of different width. Gain spectra for 2 and 12 nm wide $Ga_{0.8}In_{0.2}N/GaN$ QWs obtained for different average density in QW region are shown in Fig. 4(a) and (b), respectively. The broadening of gain peak is much larger for the wider QW due to the contribution of optical transitions between excited states. The gain intensity versus the carrier concentration is shown in Fig. 4(c). In this case it is clearly visible that for the wider QW the positive material gain appears at a lower transparency carrier concentration (n_{tr}), see arrows in Fig. 4(c), which can be directly compared with the threshold carrier concentration (n_{th}) for laser structures of the same losses on mirrors etc. This observation is in agreement with the recent experimental study for GaInN LDs [51], where lower n_{th} was observed for wider QWs. In general, this is a very interesting observation, which can strongly motivate growers to use wide QWs as the active region in LDs. The growth of such QWs can be a problem in the case of highly strained QWs for which the critical thickness is very small, but in the case of QWs with low strains the QW width can be extended up to 15 nm without any problems.

$Al_{0.8}Ga_{0.2}N/AlN$ is the material system with smaller strains comparing to $Ga_{0.8}In_{0.2}N/GaN$ system because of smaller lattice mismatch between GaN and AlN. Therefore, it is interesting to perform a very similar analysis for $Al_{0.8}Ga_{0.2}N/AlN$ QW of different width, especially as it is an interesting gain medium for UV LDs. Currently large area AlN substrates with the threading dislocation densities of $\sim 10^3$ cm^2 are available [69] and optically pumped AlGaN QW lasers emitting in deep UV can be fabricated on such substrates [70]–[74].

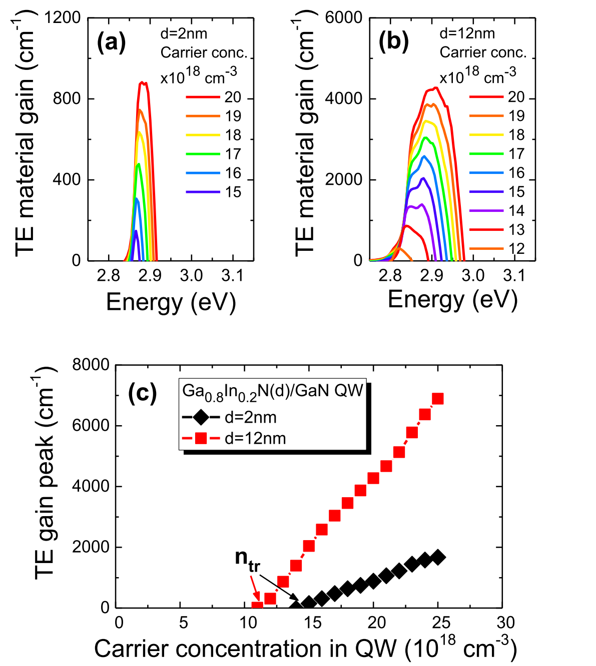

Fig. 4. Spectra of TE material gain obtained for different carrier concentrations in QW region for (a) 2 nm and (b) 12 nm wide $Ga_{0.8}In_{0.2}N/GaN$ QWs together with (c) the comparison of the peak intensity of the material gain for the two QWs of different width.

Fig. 5 shows spectra of the TM mode of the material gain calculated for $Al_{0.8}Ga_{0.2}N/AlN$ QWs of different widths at the carrier concentrations of 2.5 and 3.0×10^{19} cm^{-3}. In contrast to the $Ga_{0.8}In_{0.2}N/GaN$ QW, the fundamental transition in this QW is with TM polarization [59] and therefore the TM mode of the material gain is plotted in this figure. The change in the spectral position and the intensity of gain peak is very similar to that observed for $Ga_{0.8}In_{0.2}N/GaN$ QW. The observed quantitative differences result mainly from different energy gaps, different polarization discontinuities (i.e., built-in electric field) and different effective masses for these two QW systems. The most interesting is to analyze the difference in the built-in electric field since it is the driving force for the unusual behavior of the material gain in these QWs.

Fig. 6 shows the confinement potential for $Al_{0.8}Ga_{0.2}N/AlN$ QWs of different widths (2, 7, and 15 nm) under different carrier concentrations in QW region. Comparing to $Ga_{0.8}In_{0.2}N/GaN$ QW the built-in electric field is smaller due to smaller polarization discontinuity at the interface of $Al_{0.8}Ga_{0.2}N$ and AlN. However, despite the smaller built-in electric fields, the behavior of the confinement potential is similar to that observed for $Ga_{0.8}In_{0.2}N/GaN$ QWs. For narrow QWs, the built-in electric field cannot be fully screened, but this does not drastically affect the overlapping of the wave functions for the fundamental transition (γ is changing from 0.084 to 0.26). An increase in the QW width causes a spatial separation of electrons and holes

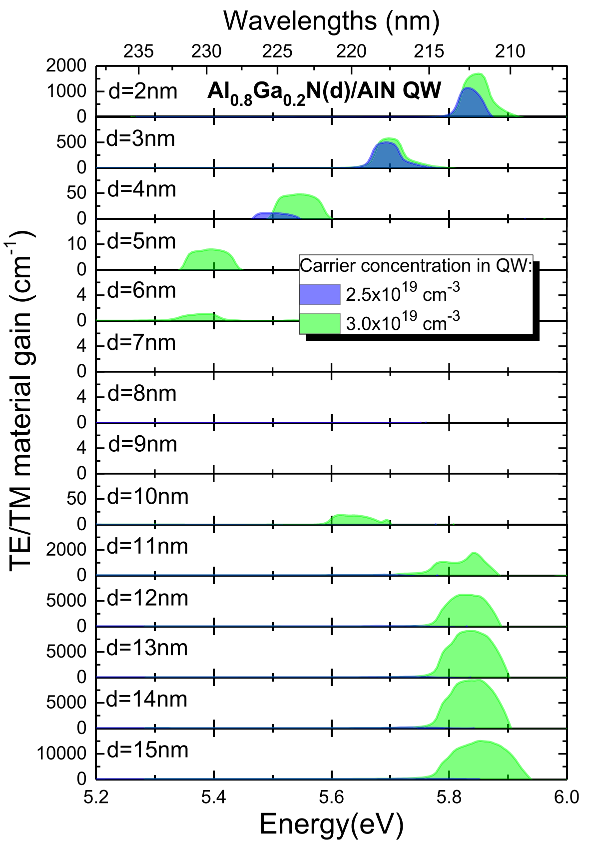

Fig. 5. TM mode of material gain for $Al_{0.8}Ga_{0.2}N(d)/GaN$ QWs of different width at carrier concentration in QW region of 2.5 and 3.0 × 10^{19} cm^{-3}. The QW width is changing from 2 to 15 nm. The two-dimensional concentration of carriers in QW going from top to bottom is as follows: 5.0, 7.5, 10.0, 12.5, 15.0, 17.5, 20.0, 22.5, 25.0, 27.5, 30.0, 32.5, 35.0, 37.5 $\times 10^{12}$ cm^{-2} for the three-dimensional carrier concentration of 2.5×10^{19} cm^{-3} and 6.0, 9.0, 12.0, 15.0, 18.0, 21.0, 24.0, 27.0, 30.0, 33.0, 36.0, 39.0, 42.0, 45.0 $\times 10^{12}$ cm^{-2} for the three-dimensional carrier concentration of 3.0×10^{19} cm^{-3}.

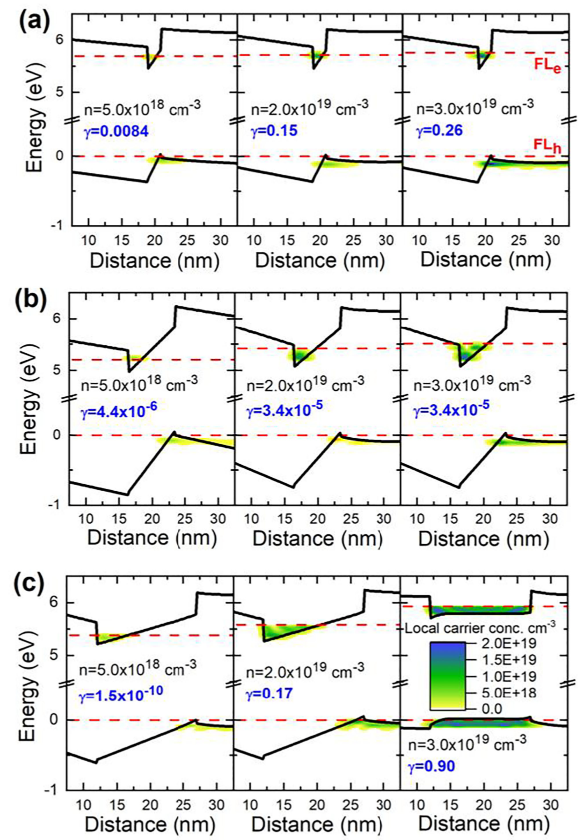

Fig. 6. The quantum confinement potential for (a) 2 nm, (b) 7 nm, and (c) 15 nm wide $Ala_{0.8}Ga_{0.2}N/AlN$ QWs obtained for different carrier concentrations in QW region. γ is the electron-hole overlap for the fundamental transition. FL_e and FL_h corresponds to the quasi Fermi level for electrons and holes, respectively. The color map shows the local carrier concentration at the appropriate energy levels. The total polarization discontinuity at the $Ala_{0.8}Ga_{0.2}N/AlN$ interface is 0.017 C/m^2 (it corresponds to the sheet concentration of 1.1×10^{13} cm^{-2}) and do not change with the QW width, while the redistribution of carriers within QWs of different width varies very significantly. The two-dimensional concentration of carriers in QW is as follows: (a) 1.0, 5.0, 6.0 $\times 10^{12}$ cm^{-2}; (b) 3.5, 17.5, 21.0 $\times 10^{12}$ cm^{-2}; (c) 7.5, 37.5, 45.0 $\times 10^{12}$ cm^{-2}.

along the growth direction and a decrease in the overlap of the wave functions for electrons and holes. The increase in carrier concentration does not help to screen the built-in electric field when the QW width is below 10 nm. Only when the QW width is greater, the screening of built-in electric field is observed and the overlap of the wave functions for the fundamental transition is large enough.

Fig. 7(a) and (b) show gain spectra for 2 and 15 nm wide $Al_{0.8}Ga_{0.2}N(d)/AlN$ QWs obtained for different carrier concentrations in QW region. The gain intensity versus the carrier concentration for the two QWs is shown in Fig. 7(c). As for $Ga_{0.8}In_{0.2}N/GaN$ QWs, it is clearly visible the broadening of gain peak is much larger for the wider QW due to the contribution of optical transitions between excited states, but the positive material gain appears at lower threshold carrier concentration for the narrow QW. For the wide QW, positive material gain appears at higher n_{tr} but grows much faster and is greater than that for narrow QW at carrier concentrations greater than $\sim 2.7\times 10^{19}$ cm^{-3}. For this narrow QW, the material gain saturates at a concentration of $\sim 2.7\times 10^{19}$ cm^{-3} and does not increase for higher concentrations of carriers in QW. Therefore, we can conclude that the growth of 15 nm wide $Al_{0.8}Ga_{0.2}N(d)/AlN$ QWs can be very favorable for LDs.

The use of both narrow and wide $Al_{0.8}Ga_{0.2}N/AlN$ QWs in electrically pumped LDs is a challenge due to the difficulties in obtaining highly conductive AlN layers [20]. It will certainly be easier for QWs with higher gallium concentration in the well and the barrier. Such QWs are not considered in this article because of the simplicity of the message to show that for polar QWs there is a certain width of the QW (the so-called ‘dead’ width), for which it is very difficult to obtain positive material gain. However similar effects are expected for $Al_{1-x}Ga_xN/Al_{1-y}Ga_yN$ QWs, which are more promising in electrically pumped UV LDs.

Fig. 8 shows a comparison of the gain intensity versus the QW width for $Ga_{0.8}In_{0.2}N/GaN$ and $Al_{0.8}Ga_{0.2}N/AlN$ QWs. For $Ga_{0.8}In_{0.2}N/GaN$ QWs the ‘dead’ width for positive material gain starts at ∼4 nm and ends at ∼8 nm. For $Al_{0.8}Ga_{0.2}N/AlN$ QW this area starts at similar width but is broader.

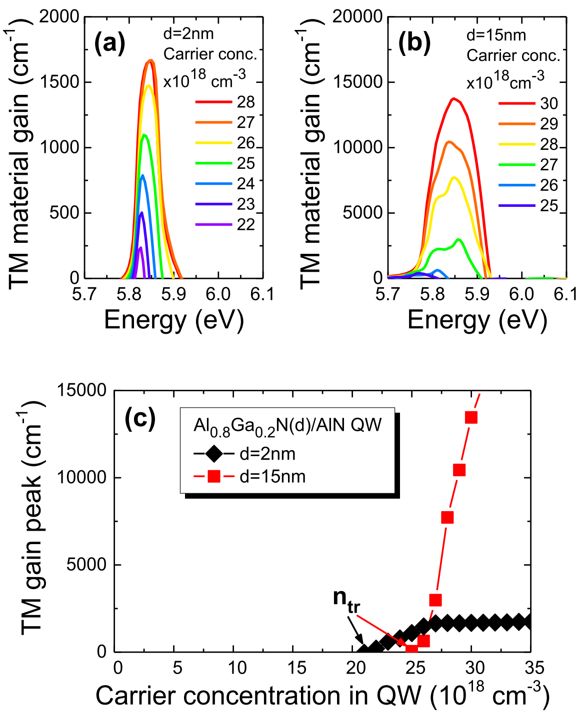

Fig. 7. Spectra of TM material gain obtained for different carrier concentrations in QW region for (a) 2 nm and (b) 15 nm wide $Al_{0.8}Ga_{0.2}N/GaN$ QWs together with (c) the comparison of the peak intensity of the material gain for the two QWs of different width.

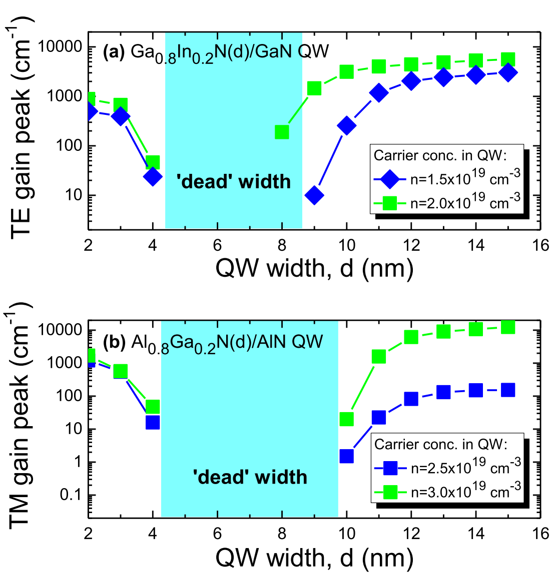

Fig. 8. Gain peak for (a) $Ga_{0.8}In_{0.2}N(d)/GaN$ and (b) $Al_{0.8}Ga_{0.2}N(d)/GaN$ QWs with the width varying in the range of 2-15 nm.

We expect that the 'dead' width will be also present for other polar III-N QWs since the built-in electric field is the driving force for no positive gain in this QW system. As can be seen in Fig. 8, the range of the "dead" width depends on the QW composition, which affects the polarization discontinuity (i.e., built-in electric field), the band gap, and the electron (hole) effective mass. A general conclusion regarding the range of 'dead' width for all polar III-N QWs is rather difficult since material parameters can vary very significantly between QWs of different composition. Moreover the comparison of the intensity of material gain for QWs of different width at the same average carrier concentration in the QW region can be insufficient for the direct extrapolation our conclusions to LDs, but the conclusion on "dead" width is still valid. It is rather obvious that narrow QWs ($d < 4$ nm) will be a good gain medium and also a good gain medium will be wide QWs ($d > 10$ nm).

In the context of studies reported in this work, the engineering of QW width in broad range can be also very interesting for staggered polar GaInN/GaN and AlGaN/AlN QWs. So far, large widths were not considered for staggered QWs as a drastic decrease in gain with increasing QW width was observed [59]. Since this polar QW system is non-intuitive, considering large widths in staggered QWs can lead to unexpected results, as shown in this paper for rectangular QWs.

III. Conclusion

In this work the material gain is calculated for $Ga_{0.8}In_{0.2}N/GaN$ and $Al_{0.8}Ga_{0.2}N/AlN$ QWs with the width varying in the range of 2-15 nm. We observed that the material gain for these QWs drops to zero with the increase in the QW width and reaches negative values in the width range of ∼4-8 nm even for high carrier concentrations, but after exceeding a certain width to 8-12 nm it begins to increase rapidly and reaches the values greater than those observed for narrow wells. This phenomenon is related to the screening of the built-in electric field by carriers, which is easier for wide QWs, and the reduction of the distance between the energy levels for electrons and holes. For the latter reason, optical transitions between higher energy states make a very significant contribution to the positive material gain.

References

[1] F. Bernardini and V. Fiorentini, "Nonlinear macroscopic polarization in III-V nitride alloys," *Phys. Rev. B*, vol. 64, 2001, Art. no. 085207.
[2] O. Ambacher *et al.*, "Pyroelectric properties of Al(In)GaN/GaN hetero- and quantum well structures," *J. Phys.: Condens. Matter*, vol. 14, 2012, Art. no. 3399.
[3] M. Asif Khan, A. Bhattarai, J. N. Kuznia, and D. T. Olson, "High electron mobility transistor based on a GaN-$Al_xGa_{1-x}N$ heterojunction," *Appl. Phys. Lett.*, vol. 63, 1993, Art. no. 1214.
[4] O. Ambacher *et al.*, "Two-dimensional electron gases induced by spontaneous and piezoelectric polarization charges in N- and Ga-face AlGaN/GaN heterostructures," *J. Appl. Phys.*, vol. 85, 1999, Art. no. 3222.
[5] O. Ambacher *et al.*, "Two dimensional electron gases induced by spontaneous and piezoelectric polarization in undoped and doped AlGaN/GaN heterostructures," *J. Appl. Phys.*, vol. 87, 2000, Art. no. 334.
[6] J. P. Ibbetson *et al.*, "Polarization effects, surface states, and the source of electrons in AlGaN/GaN heterostructure field effect transistors," *Appl. Phys. Lett.*, vol. 77, 2000, Art. no. 250.
[7] J. Simon, V. Protasenko, C. Lian, H. Xing, and D. Jena, "Polarization-induced hole doping in wide–band-gap uniaxial semiconductor heterostructures," *Science*, vol. 327, 2010, Art. no. 60.
[8] J. Simon *et al.*, "Polarization-induced zener tunnel junctions in wide-band-gap heterostructures," *Phys. Rev. Lett.*, vol. 103, 2009, Art. no. 026801.
[9] S. Krishnamoorthy *et al.*, "Polarization-engineered GaN/InGaN/GaN tunnel diodes," *Appl. Phys. Lett.*, vol. 97, 2010, Art. no. 203502.
[10] J. Encomendero *et al.*, "New tunneling features in polar III-nitride resonant tunneling diodes," *Phys. Rev. X*, vol. 7, 2017, Art. no. 041017.
[11] S. Nakamura, G. Fasol, and S. Pearton, "*The Blue Laser Diode: The Complete Story*," Berlin, Germany: Springer-Verlag, 2000.

[12] M. R. Krames *et al.*, "Status and future of high-power light-emitting diodes for solid-state lighting," *J. Disp. Technol.*, vol. 3, 2007, Art. no. 160.

[13] M. H. Crawford, "LEDs for solid-state lighting: Performance challenges and recent advances," *IEEE J. Sel. Topics Quantum Electron.*, vol. 15, no. 4, pp. 1028–1040, Jul./Aug. 2009.

[14] S. Pimputkar, J. S. Speck, S. P. DenBaars, and S. Nakamura, "Prospects for LED lighting," *Nat. Photon.*, vol. 3, 2009, Art. no. 180.

[15] A. Khan, K. Balakrishnan, and T. Katona, "Ultraviolet light-emitting diodes based on group three nitrides," *Nat. Photon*, vol. 2, 2008, Art. no. 77.

[16] H. Yoshida, M. Kuwabara, Y. Yamashita, K. Uchiyama, and H. Kan, "The current status of ultraviolet laser diodes," *Phys. Status Solidi A*, vol. 208, 2011, Art. no. 1586.

[17] H. Hirayama, N. Maeda, S. Fujikawa, S. Toyoda, and N. Kamata, "Recent progress and future prospects of algan-based high-efficiency deep-ultraviolet light-emitting diodes," *Jpn. J. Appl. Phys.*, vol. 53, 2014, Art. no. 100209.

[18] M. Kneissl, "III-nitride ultraviolet emitters - technology and applications," in *Springer Series in Materials Science* J. Rass, eds., vol. 227, Berlin, Germany: Springer-Verlag, 2016.

[19] D. B. Li, K. Jiang, X. J. Sun, and C. L. Guo, "AlGaN photonics: Recent advances in materials and ultraviolet devices," *Adv. Opt. Photon.*, vol. 10, 2018, Art. no. 43.

[20] H. Amano *et al.*, "The 2020 UV emitter roadmap," *J. Phys. D: Appl. Phys.*, vol. 53, 2020, Art. no. 503001.

[21] Y. Gerchman, H. Mamane, N. Friedman, and M. Mandelboim, "UV-LED disinfection of coronavirus: Wavelength effect," *J. Photochemistry Photobiol. B: Biol.*, vol. 212, 2020, Art. no. 112044.

[22] S. Kamiyama *et al.*, "UV laser diode with 350.9-nm-lasing wavelength grown by hetero-epitaxial-lateral overgrowth technology," *IEEE J. Sel. Topics Quant. Electron.*, vol. 11, no. 5, 2005, Art. no. 1069.

[23] H. Yoshida, Y. Yamashita, M. Kuwabara, and H. Kan, "A 342-nm ultraviolet AlGaN multiple-quantum-well laser diode," *Nat. Photon.*, vol. 2, 2008, Art. no. 551.

[24] H. Yoshida, Y. Yamashita, M. Kuwabara, and H. Kan, "Demonstration of an ultraviolet 336 nm AlGaN multiple-quantum-well laser diode," *Appl. Phys. Lett.*, vol. 93, 2008, Art. no. 241106.

[25] K. H. Li, X. Liu, Q. Wang, S. Zhao, and Z. Mi, "Ultralow-threshold electrically injected AlGaN nanowire ultraviolet lasers on Si operating at low temperature," *Nat. Nanotechnol.*, vol. 10, 2015, Art. no. 140.

[26] Z. Zhang *et al.*, "A 271.8 nm deep-ultraviolet laser diode for room temperature operation," *Appl. Phys. Exp.*, vol. 12, 2019, Art. no. 124003.

[27] H. Taketomi *et al.*, "Over 1 W record-peak-power operation of a 338 nm AlGaN multiple-quantum-well laser diode on a GaN substrate," *Jpn. J. Appl. Phys.*, vol. 55, 2016, Art. no. 05FJ05.

[28] T. Takeuchi *et al.*, "Quantum-confined stark effect due to piezoelectric fields in GaInN strained quantum wells," *Jpn. J. Appl. Phys.*, vol. 36, 1997, Art. no. L382.

[29] J. Seo Im *et al.*, "Reduction of oscillator strength due to piezoelectric fields in GaN/$Al_xGa_{1-x}N$ quantum wells," *Phys. Rev. B*, vol. 57, 1998, Art. no. R9435.

[30] M. Leroux *et al.*, "Quantum confined stark effect due to built-in internal polarization fields in (Al, Ga)N/GaN quantum wells," *Phys. Rev. B*, vol. 58, 1998, Art. no. R13371.

[31] R. Langer *et al.*, "Giant electric fields in unstrained GaN single quantum wells," *Appl. Phys. Lett.*, vol. 74, 1999, Art. no. 3827.

[32] V. Fiorentini, F. Bernardini, F. D. Sala, A. Di Carlo, and P. Lugli, "Effects of macroscopic polarization in III-V nitride multiple quantum wells," *Phys. Rev. B*, vol. 60, 1999, Art. no. 8849.

[33] F. D. Sala *et al.*, "Free-carrier screening of polarization fields in wurtzite GaN/InGaN laser structures," *Appl. Phys. Lett.*, vol. 74, 1999, Art. no. 2002.

[34] N. Grandjean *et al.*, "Built-in electric-field effects in wurtzite AlGaN/GaN quantum wells," *J. Appl. Phys.*, vol. 86, 1999, Art. no. 3714.

[35] Y. C. Shen *et al.*, "Auger recombination in InGaN measured by photoluminescence," *Appl. Phys. Lett.*, vol. 91, 2007, Art. no. 141101.

[36] M.-H. Kim *et al.*, "Origin of efficiency droop in gan-based light-emitting diodes," *Appl. Phys. Lett.*, vol. 91, 2007, Art. no. 183507.

[37] J. Piprek, "Efficiency droop in nitride-based light-emitting diodes," *Phys. Status Solidi A*, vol. 207, 2010, Art. no. 2217.

[38] E. Kioupakis, P. Rinke, K. T. Delaney, and C. G. Van de Walle, "Indirect auger recombination as a cause of efficiency droop in nitride light-emitting diodes," *Appl. Phys. Lett.*, vol. 98, 2011, Art. no. 161107.

[39] J. Iveland, L. Martinelli, J. Peretti, J. S. Speck, and C. Weisbuch, "Direct measurement of auger electrons emitted from a semiconductor light-emitting diode under electrical injection: Identification of the dominant mechanism for efficiency droop," *Phys. Rev. Lett.*, vol. 110, 2013, Art. no. 177406.

[40] M. Auf der Maur, A. Pecchia, G. Penazzi, W. Rodrigues, and A. Di Carlo, "Efficiency drop in green InGaN/GaN light emitting diodes: The role of random alloy fluctuations," *Phys. Rev. Lett.*, vol. 116, 2016, Art. no. 027401.

[41] J. Xie *et al.*, "Lasing and longitudinal cavity modes in photo-pumped deep ultraviolet AlGaN heterostructures," *Appl. Phys. Lett.*, vol. 102, 2013, Art. no. 171102.

[42] Z. Lochner *et al.*, "Deep-ultraviolet lasing at 243 nm from photo-pumped AlGaN/AlN heterostructure on AlN substrate," *Appl. Phys. Lett.*, vol. 102, 2013, Art. no. 101110.

[43] W. Guo *et al.*, "Stimulated emission and optical gain in AlGaN heterostructures grown on bulk AlN substrates," *J. Appl. Phys.*, vol. 115, 2014, Art. no. 103108.

[44] M. Martens *et al.*, "Performance characteristics of UV-C algan-based lasers grown on sapphire and bulk AlN substrates," *IEEE Phot. Technol. Lett.*, vol. 26, no. 4, pp. 342–345, Feb. 2014.

[45] M. Gladysiewicz, M. Rudzinski, D. Hommel, and R. Kudrawiec, "Emission and material gain spectra of polar compressive strained AlGaN quantum wells grown on virtual AlGaN substrates: Tuning emission wavelength and mixing TE and TM mode of light polarization," *Semicond. Sci. Technol.*, vol. 33, 2018, Art. no. 075003.

[46] Y. Imajo, A. Kasukawa, T. Namegaya, and T. Kikuta, "1.3 μm $InAs_yP_{1-y}$/InP strained-layer quantum well laser diodes grown by metalorganic chemical vapor deposition," *Appl. Phys. Lett.*, vol. 61, 1992, Art. no. 2506.

[47] M. Grau, C. Lin, O. Dier, C. Lauer, and M.-C. Amann, "Room-temperature operation of 3.26 μm GaSb-based type-I lasers with quinternary AlGaInAsSb barriers," *Appl. Phys. Lett.*, vol. 87, 2005, Art. no. 241104.

[48] M. Yamada *et al.*, "Low-threshold operation of 1.3-mu m GaAsSb quantum-well lasers directly grown on GaAs substrates," *IEEE Phot. Tech. Lett.*, vol. 12, no. 7, pp. 774–776, Jul. 2000.

[49] S. R. Bank *et al.*, "Recent progress on 1.55-μm dilute-nitride lasers," *IEEE J. Quantum Electon.*, vol. 43, no. 9, pp. 773–785, Sep. 2007.

[50] G. Muziol *et al.*, "Beyond quantum efficiency limitations originating from the piezoelectric polarization in light-emitting devices," *ACS Photon.*, vol. 6, 2019, Art. no. 1963.

[51] G. Muziol *et al.*, "Optical properties of III-nitride laser diodes with wide InGaN quantum wells," *Appl. Phys. Exp.*, vol. 12, 2019, Art. no. 072003.

[52] S. L. Chuang, "Optical gain of strained wurtzite GaN quantum-well lasers," *IEEE J. Quantum Electron.*, vol. 32, no. 10, pp. 1791–1800, Oct. 1996.

[53] Y. C. Yeo, T. C. Chong, M.-F. Li, and W. J. Fan, "Electronic band structures and optical gain spectra of strained wurtzite GaN–$Al_xGa_{1-x}N$ quantum-well lasers," *IEEE J Quantum Electron.*, vol. 34, no. 3, 1998, Art. no. 526.

[54] V. I. Litvinov, "Optical transitions and gain in group-III nitride quantum wells," *J Appl. Phys.*, vol. 88, 2000, Art. no. 5814.

[55] W. W. Chow and M. Kneissl, "Laser gain properties of AlGaN quantum wells," *J. Appl. Phys.*, vol. 98, 2005, Art. no. 114502.

[56] W. G. Scheibenzuber, U. T. Schwarz, R. G. Veprek, B. Witzigmann, and A. Hangleiter, "Calculation of optical eigenmodes and gain in semipolar and nonpolar InGaN/GaN laser diodes," *Phys. Rev. B*, vol. 80, 2009, Art. no. 115320.

[57] H. Zhao and N. Tansu, "Optical gain characteristics of staggered InGaN quantum wells lasers," *J. Appl. Phys.*, vol. 107, 2010, Art. no. 113110.

[58] T. Oto, R. G. Banal, M. Funato, and Y. Kawakami, "Optical gain characteristics in Al-rich AlGaN/AlN quantum wells," *Appl. Phys. Lett.*, vol. 104, 2014, Art. no. 181102.

[59] M. Gladysiewicz, D. Hommel, and R. Kudrawiec, "Material gain engineering in staggered polar AlGaN/AlN quantum wells dedicated for deep UV lasers," *IEEE J. Sel. Topics Quantum Electron.*, vol. 25, no. 6, pp. 1–8, Nov./Dec. 2019, Art no. 1901108.

[60] B. Witzigmann *et al.*, "Calculation of optical gain in AlGaN quantum wells for ultraviolet emission," *AIP Adv.*, vol. 10, 2020, Art. no. 095307.

[61] S. L. Chuang and C. S. Chang, "k·p method for strained wurtzite semiconductors," *Phys. Rev. B*, vol. 54, 1996, Art. no. 2491.

[62] S. L. Chuang and C. S. Chang, "A band-structure model of strained quantum-well wurtzite semiconductors," *Semicond. Sci. Technol.*, vol. 12, 1997, Art. no. 252.

[63] S.-H. Park and S.-L. Chuang, "Crystal-orientation effects on the piezoelectric field and electronic properties of strained wurtzite semiconductors," *Phys. Rev. B*, vol. 59, 1999, Art. no. 4725.

[64] I. Vurgaftman and J. R. Meyer, "Band parameters for nitrogen-containing semiconductors," *J. Appl. Phys.*, vol. 94, 2003, Art. no. 3675.
[65] G. L. Bir and G. E. Pikus, "*Symmetry and Strain Effects in Semiconductors*," Hoboken, NJ, USA: (John) Wiley (& Sons,), New York, NY, USA, 1974.
[66] R. Kudrawiec and D. Hommel, "Bandgap engineering in III-nitrides with boron and group V elements: Toward applications in ultraviolet emitters," *Appl. Phys. Rev.*, vol. 7, 2020, Art. no. 041314.
[67] C. E. Dreyer, A. Janotti, C. G. Van de Walle, and D. Vanderbilt, "Correct 'Implementation of polarization constants in wurtzite materials and impact on III-nitrides," *Phys. Rev. X*, vol. 6, 2016, Art. no. 021038.
[68] A. Fischer, H. Kühne, and H. Richter, "New approach in equilibrium theory for strained layer relaxation," *Phys. Rev. Lett.*, vol. 73, 1994, Art. no. 2712.
[69] "AlN substrate products," [Online]. Available: http://www.hexatechinc.com/aln-wafer-sales.html
[70] Z. Bryan *et al.*, "High internal quantum efficiency in AlGaN multiple quantum wells grown on bulk AlN substrates," *Appl. Phys. Lett.*, vol. 106, 2015, Art. no. 142107.
[71] J. Xie *et al.*, "Lasing and longitudinal cavity modes in photo-pumped deep ultraviolet AlGaN heterostructures," *Appl. Phys. Lett.*, vol. 102, 2013, Art. no. 171102.
[72] Z. Lochner *et al.*, "Deep-ultraviolet lasing at 243 nm from photo-pumped AlGaN/AlN heterostructure on AlN substrate," *Appl. Phys. Lett.*, vol. 102, 2013, Art. no. 101110.
[73] W. Guo *et al.*, "Stimulated emission and optical gain in AlGaN heterostructures grown on bulk AlN substrates," *J. Appl. Phys.*, vol. 115, 2014, Art. no. 103108.
[74] M. Martens *et al.*, "Performance characteristics of UV-C AlGaN-Based lasers grown on sapphire and bulk AlN substrates," *IEEE Photon. Technol. Lett.*, vol. 26, no. 4, pp. 342–345, Feb. 2014.

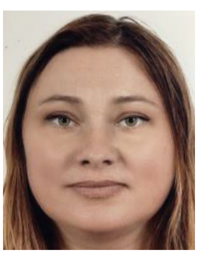

Marta Gladysiewicz received the M.S. (Hons.) and Ph.D. (Hons.) degrees in physic from the Wroclaw University of Science and Technology (WUST), Wroclaw, Poland, in 1999 and 2003, respectively. Her M.S. and Ph.D. thesis were devoted to high temperature superconductors. Since 2005, her scientific activity is focused on novel semiconductor materials, including dilute nitrides, dilute bismidies, and III-Nitrides. Since 2007, she has been an Assistant Professor with the Institute of Physics, WUST. Since 2016, she has been a Professor with WUST. Her current research interests include theoretical investigations of the band structure and optical properties of III–V group materials and their low-dimensional structures. She was a short term Visiting Researcher with Wilfrid Laurier University, Waterloo, ON, Canada (2011 and 2014), and the Lawrence Berkeley National Laboratory, Berkeley, CA, USA (2012 and 2013), where her research activity was focused on theoretical calculations of the band structure for dilute nitrides. Prof. Gladysiewicz was the recipient of the Student Award from Polish Ministry of Science and Higher Education (1999). Her scientific activity was awarded by four grants from National Science Center, Poland.

Czesław Skierbiszewski received the M.S. and Ph.D. degrees in physics from Warsaw University, Warsaw, Poland, in 1984 and the Institute of Physics Polish Academy of Sciences (IP PAS), Warsaw, in 1993, respectively, and the D.Sc. (Habilitation) degree in physics from IP PAS, in 2006. From 1993 to 1995, he was a Postdoctoral Scholar with University of Montpellier, Montpellier, France, and University of Linz, Linz, Austria, where his researches were related to weak localization in asymmetric quantum wells and the metastable states in GaAs. He was also interested in experimental determination of band structure of diluted nitrides. Since 2002, he has been the Head of the Molecular Beam Epitaxy (MBE) Group, Institute of High Pressure Physics PAS (IHPP PAS), focusing on epitaxy of nitride laser diodes by plasma assisted MBE. Since 2015, he has been a Full Professor with IHPP PAS.

Robert Kudrawiec received the M.S. and Ph.D. (Hons.) degrees in physics from the Wrocław University of Science and Technology (WUST), Poland, in 2000 and 2004, respectively, and the D.Sc. (Habilitation) degree in physics from the Institute of Physics, WUST, in 2010. His Ph.D. thesis was devoted to dilute nitrides. During the M.S. and Ph.D. studies, he focused on applications of the modulation spectroscopy to investigate the band structure of low dimensional systems. From 2006 to 2007, he was a Postdoctoral Scholar with Stanford University, Stanford, CA, USA, where his research was centered on the band structure and defects in GaInNAsSb–GaAs materials. From 2012 to 2013, he was a Researcher with Lawrence National Berkeley Laboratory, Berkeley, CA, USA, where his activity was focused on novel III–V and II–VI materials dedicated for solar cell applications. Since 2018, he has been a Full Professor with the Faculty of Fundamental Problems of Technology, WUST. He has coauthored more than 300 publications in refereed journals in his research areas. His current research interests include the application of photoreflectance, contactless electroreflectance, micro-photoluminescence, and time resolved photoluminescence spectroscopies to investigate the optical properties of GaN-, GaAs-, InP-, and GaSb-based materials and low dimensional structures, and recently van der Waals crystals and perovskites. Since 2017, he has been associated with the Polish Center for Technology Development at Wroclaw, where he is working on UV light emitters.